Article

pubs.acs.org/Biomac

Photopatterning of Hydrogel Microarrays in Closed Microchips

Burcu Gumuscu,* Johan G. Bomer, Albert van den Berg, and Jan C. T. Eijkel*

BIOS Lab-on-a-Chip Group, MESA+ Institute for Nanotechnology, MIRA Institute for Biomedical Technology and Technical Medicine, University of Twente, Enschede, The Netherlands

Supporting Information

ABSTRACT: To date, optical lithography has been extensively used for in situ patterning of hydrogel structures in a scale range from hundreds of microns to a few millimeters. The two main limitations which prevent smaller feature sizes of hydrogel structures are (1) the upper glass layer of a microchip maintains a large spacing (typically 525 μm) between the photomask and hydrogel precursor, leading to diffraction of UV light at the edges of mask patterns, (2) diffusion of free radicals and monomers results in irregular polymerization near the illumination interface. In this work, we present a simple approach to enable the use of optical lithography to fabricate hydrogel arrays with a minimum feature size of 4 μm inside closed microchips. To achieve this, we combined two different techniques. First, the upper glass layer of the microchip was thinned by mechanical polishing to reduce the spacing between the photomask and hydrogel precursor, and thereby the diffraction of UV light at the edges of mask patterns. The polishing process reduces the upper layer thickness from ~525 to ~100 μm, and the mean surface roughness from 20 to 3 nm. Second, we developed an intermittent illumination technique consisting of short illumination periods followed by relatively longer dark periods, which decrease the diffusion of monomers. Combination of these two methods allows for fabrication of 0.4×10^6 sub-10 μm sized hydrogel patterns over large areas (cm^2) with high reproducibility (~98.5% patterning success). The patterning method is tested with two different types of photopolymerizing hydrogels: polyacrylamide and polyethylene glycol diacrylate. This method enables in situ fabrication of well-defined hydrogel patterns and presents a simple approach to fabricate 3-D hydrogel matrices for biomolecule separation, biosensing, tissue engineering, and immobilized protein microarray applications.

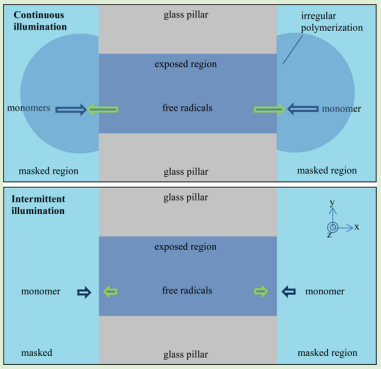

1. INTRODUCTION

In the last decades, hydrogels have attracted a great deal of attention in numerous biotechnological applications due to their hydrophilic porous network, biocompatibility, and highly tunable nature. These properties enable the transport of molecules throughout the material and maintain tailorable matrices to accommodate cells.[1] Hydrogels can also respond to their close environment due to their excellent sensitivity to pH,[2] ionic strength,[2] temperature,[3,4] electric field,[5−7] and light.[8] These functionalities have brought hydrogels into the class of smart materials and have led to their widespread use in various biological applications. Reddy et al. used hydrogels for protein crystallization to evaluate their selectivity on different biomolecules,[9] while Paustian et al. fabricated microwindow hydrogels and used their local electric permeability to sculpt electric fields in a microfluidic chip.[10] In another study, macrophage cells were encapsulated in hydrogel patterns in order to detect enzymatic reactions.[11] Ashley et al. demonstrated that patterned hydrogels can be used as tunable drug release tools[12] and Byun et al. studied integration of three-dimensional protein arrays into a hydrogel matrix for conversion of DNA arrays into three-dimensional protein arrays.[13] Suzuki et al. reported the UV light sensitivity of hydrogel structures, which can be used as photoresponsive artificial muscles and memory devices.[14]

Integrating hydrogel arrays into closed microchips is beneficial for numerous microfluidic applications owing to their capacity to handle small sample volumes and to perform in-parallel analyses.[15−17] Hydrogel arrays consisting of small-volume subunits enable faster mass transport and provide higher surface-to-volume ratios, which are essential to increase the sample throughput and number of analyses. Although the microfabrication of hydrogel arrays on rigid substrates has been extensively investigated, the ability to do the same in closed microchips has not been sufficiently examined. For the fabrication of patterned hydrogels on the microscale, a variety of techniques have been used, including 3D printing,[18] soft-lithography,[19] multiphoton lithography,[20] and optical lithography.[21] In 3D printing, hydrogel structures are built up by layer-by-layer deposition via consecutive lithographic steps.[22] Despite the promise of accurate and fast fabrication, 3D printing provides a poor degree of control over the size distribution of hydrogel structures, which are typically in a scale range from hundreds of microns to tens of millimeters.[22] Soft lithography techniques, including microcontact printing[23] and micromolding,[24] offer inexpensive, convenient, and scalable templates for patterning. However, the usage of polymer molds

Received: August 15, 2015
Revised: November 6, 2015
Published: November 11, 2015

DOI: 10.1021/acs.biomac.5b01104
Biomacromolecules 2015, 16, 3802−3810

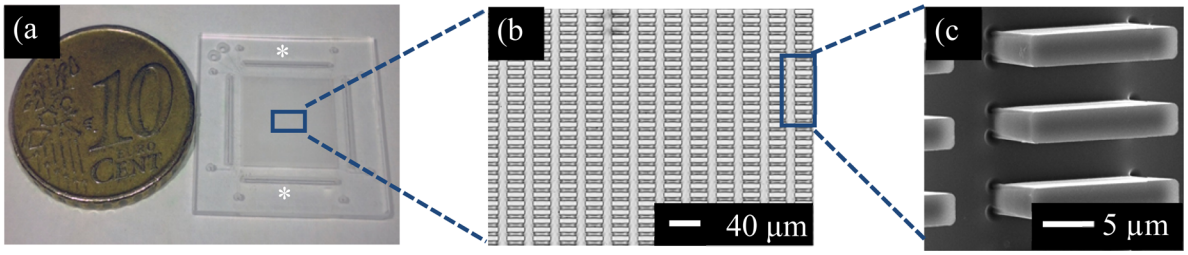

Figure 1. (a) An image of the microchip with glass pillars and microfluidic inlets and outlets (*). (b) Optical microscopy image of glass pillar array (light colored rectangles) and air-filled channels (darker colored areas). (c) Tilted top view of glass pillars under SEM. The depth, width, and length of pillars are 20 × 20 × 5 μm, respectively.

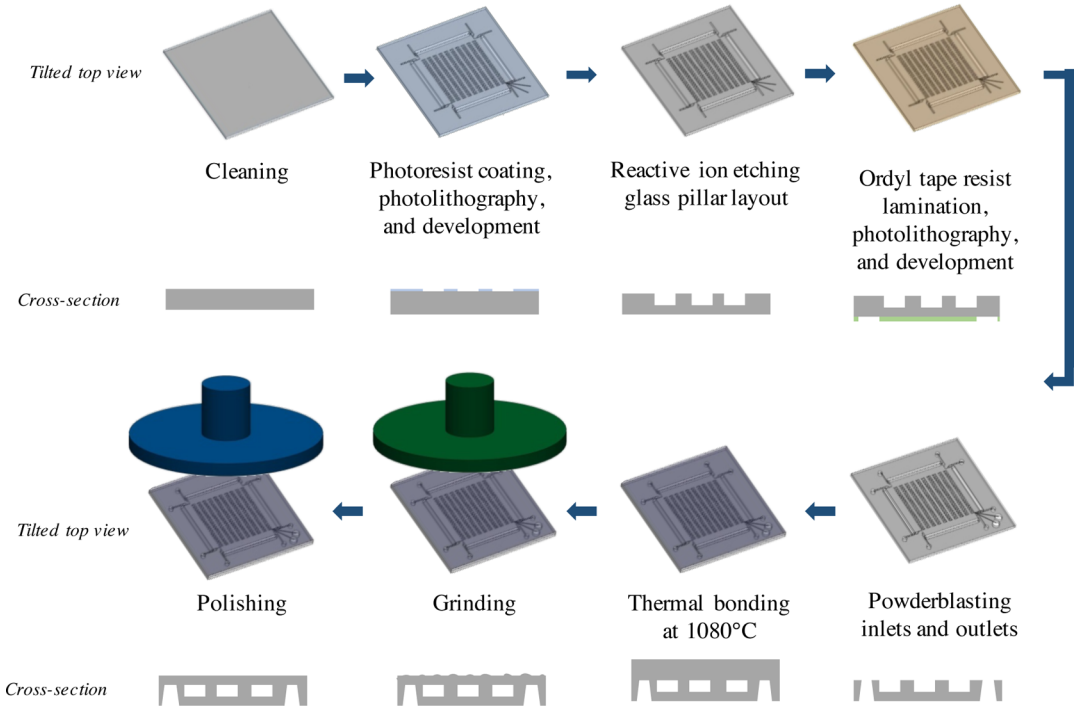

Figure 2. Schematic illustration of microchip fabrication. The sketches on the bottom part present the vertical cross-section of the microchannels.

is unsuitable to pattern hydrogels in closed microchips.[25] Multiphoton lithography[20] is known for providing high resolution patterns; on the other hand, complexity of the setup and low area coverage are the main drawbacks of this technique. Masked photolithography[7,26,27] and laser patterning[28] are the most preferred optical lithography techniques, which are well-established and have proven to be reliable for patterning hydrogel arrays. When it comes to in situ patterning of very small feature sizes using optical lithography; however, the resolution turns out to be rather poor compared to the resolution obtained on open rigid surfaces. One problem with the resolution is the UV diffraction caused by the thickness of the upper glass layer (typically 525 μm), which maintains a large spacing between the photomask and hydrogel precursor. A second problem is the high diffusion rates of monomers and free radicals under flood illumination, leading to structures with indistinct edges.[29] As a result, the current state of these techniques cannot satisfy the requirements of emerging applications which call for the use of in situ patterned hydrogel arrays with feature size of a few microns.

Previously, our group has introduced the capillary pinning technique for autonomous fabrication of picoliter-volume microarrays of both photopolymerizing and thermogelling hydrogels in closed microchips.[30] Glass obstacles (capillary barriers) were fabricated in microchannels for local pinning of the hydrogel precursor, yielding periodic hydrogel patterns over a 1 cm^2 area. Even though the capillary pinning technique is promising, alternative and simple fabrication processes to integrate hydrogel microarrays in closed microchips would still be beneficial. Here we report the fabrication of periodic hydrogel structures in a fused silica microchip enabled by optical lithography. After bonding two glass layers of the microchip, the upper layer was ground and polished to reduce its thickness and roughness. This, in combination with an illumination recipe developed to enhance hydrogel boundary definition, allowed us to precisely control the photopatterning of hydrogel microarrays over large areas (cm^2) with sub-10 μm feature size and up to 98.5% success. For proof-of-concept demonstration, we fabricated a closed microchip with an array of 0.4 × 10^6 hydrogel patterns sandwiched between glass pillars using 0.5 μL of hydrogel precursor. Our approach greatly simplifies hydrogel integration into microchips, as the microarrays are fabricated in situ and can be used with multiple types of photopolymerizing hydrogels.

DOI: 10.1021/acs.biomac.5b01104
Biomacromolecules 2015, 16, 3802−3810

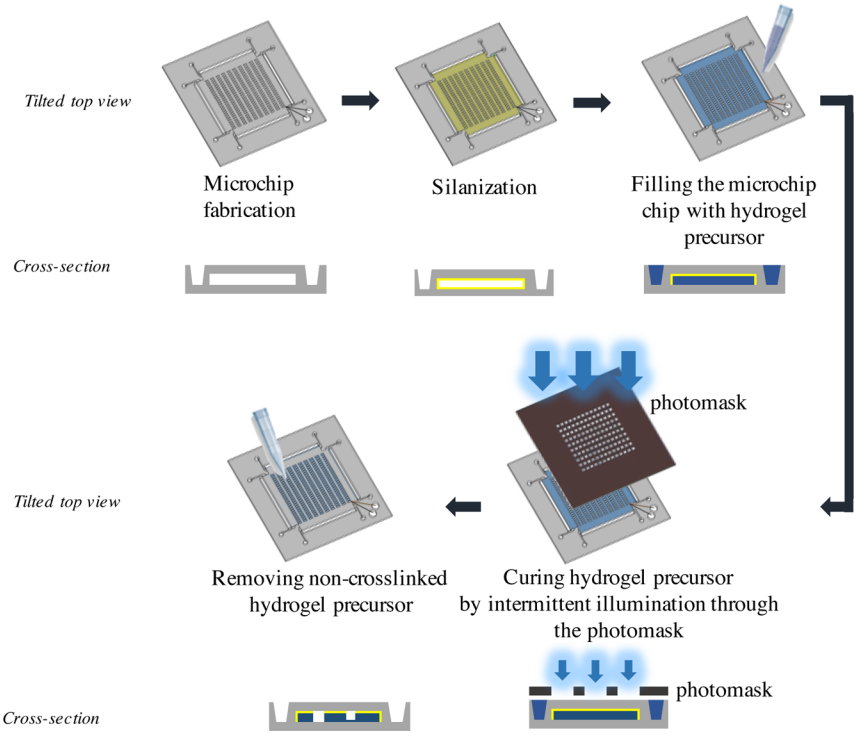

Figure 3. Process flow for pattering micron-sized hydrogels in a closed microchip. Sketches on the bottom part present the vertical cross-section of the microchannels. Yellow lines present silanized glass surfaces, light blue areas are non-cross-linked hydrogel precursors, and dark blue colored areas are cross-linked hydrogels.

2. METHODS

2.1. Microchip Fabrication. The microchips were fabricated in the MESA+ cleanroom facility at the University of Twente and consisted of two 525 μm thick layers of fused silica. The upper layer contained glass pillar array, microfluidic channels, fluidic inlets, and fluidic outlets, while the lower layer was not processed. Figure 1 shows an assembled microchip containing glass pillar array. We used standard reactive ion etching (RIE) for the fabrication of the glass pillars and microfluidic channels on the upper layer (Figure 2). Before the RIE process, the upper layer was spin-coated with a negative photoresist (SU-8 2050, MicroChem Inc.) to protect the underlying layer from etching. An optical lithography step was then performed to pattern the pillars and microfluidic channels, which were subsequently postbaked and developed before etching by RIE. The SU-8 layer was then stripped in a piranha bath. Etched channels were ~20 μm deep, as measured using the Dektak 150 Surface Profiler (Bruker). Scanning electron microscopy (SEM) images of the etched structures were taken using a JEOL JSM 5610 (Jeol Inc.) field emission scanning electron microscope. Fluidic inlets and outlets were powder blasted on the backside of the upper layer using an Ordyl tape resist (BF410; Tokyo Ohka Kogyo) for masking. After lamination and optical lithography, the tape resist was developed using 1% of $NaHCO_3$ and subsequently removed by acetone once the powder blasting process was completed. Finally, the processed layer was cleaned and thermally bonded with a plain fused silica layer at 1080 °C.

2.2. Grinding and Polishing. The upper layer of the microchip was laminated with a protection tape to avoid clogging of microchannels during the grinding and polishing processes. The microchip was placed in an Engis 15 grinding and polishing tool consisting of diamond cup wheels, a porous ceramic chuck, and a vacuum holder. Silicon carbide particles (particle sizes: 280, 400, 800, and 1000 μm) were mixed with deionized water for the grinding process. Surface roughness was reduced by polishing the lower layer using Kemet Vloeistof Type K solution (Kemet Inc.), which consisted of water-treated light oil and surface-modified silica particles. The microchip was subsequently cleaned with deionized water and the protection tape was removed.

2.3. Fabrication of Hydrogel Structures. *2.3.1. Surface Silanization.* Microchannels were silanized to enable the formation of covalent bonds between the glass layer and the hydrogel. First, the microchip was cleaned in 0.1 M NaOH for 30 min in an ultrasonic bath. Microchannels were then rinsed with deionized water and placed in a solution of 2:3:5 (v/v/v) 3-trimethoxysilylpropyl methacrylate (Sigma)/glacial acetic acid (Sigma)/deionized water for 60 min. Finally, the microchip was rinsed with acetone for 1 min, then with deionized water for 2 min, and dried at 110 °C for 7 min to promote covalent siloxane bond formation on the glass layer.[31]

2.3.2. Preparation of Hydrogels. It is crucial to take the next experimental step immediately after finishing the previous one during preparation and polymerization of hydrogel precursors, since >1 min waiting times can influence the degree of oxygenation and, therefore, polymerization. Milli-Q water was used in all experiments. All solutions were degassed under 92 kPa vacuum for an hour immediately prior to use. Polyacrylamide precursor was prepared in a N_2 containing environment by blending 20% v/v of acrylamide/bis (19:1; BioRad), 2% w/v of 2,2-dimethoxy-2-phenylacetophenone (DMPA, Invitrogen), and 2% w/v of ammonium persulfate (Invitrogen) solutions in a fume hood to avoid dust particles. Patterning and polymerization were also performed in a N_2 containing environment, because the cross-linking reaction is quenched by O_2. Concentration of O_2 was measured using an oximeter (GMH 3691, Greisinger) and >1% O_2 was observed to inhibit the polymerization reaction. It is possible to replace N_2 with Ar when polymerizing polyacrylamide. Polymerization did not occur when 1 mL of each solution was not degassed for less than 1 h. Polyethylene glycol diacrylate (PEG DA) (MW 3400; Laysan Bio Inc.) precursor was prepared in a fume hood by dissolving the PEG DA powder in 15% w/v of PBS solution and blending the final mixture with 10% w/v of 2-hydroxy-1[4-(2-hydroxyethoxy)-phenyl]-2-methyl-1-propane (Irgacure 2959; Sigma) in ethanol solution. The molar fraction of the PEG DA monomer was 15%, while that of the Irgacure was 85%. A high molar fraction of the photoinitiator was used to maintain the polymerization yield at 365 nm wavelength. Possible contact with light was avoided during the preparation of PEG DA precursor solution. All

DOI: 10.1021/acs.biomac.5b01104
Biomacromolecules 2015, 16, 3802−3810

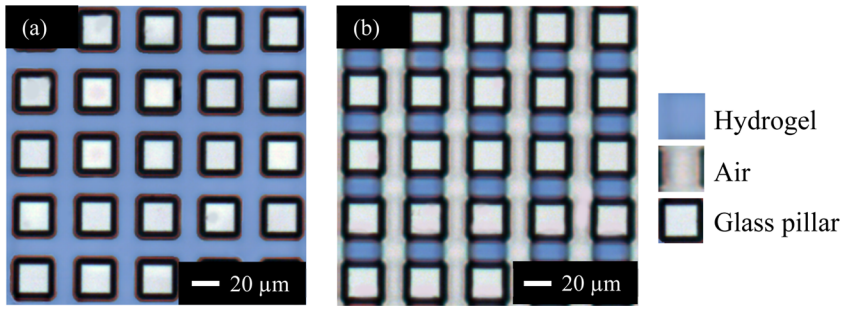

Figure 4. Phase contrast microscopy image of photopolymerized polyacrylamide hydrogel. Gray squares are glass pillars and blue rectangles are hydrogels. (a) Photopolymerization by 10 min flood exposure and (b) photopolymerization by 10 min UV exposure with 2 s on 4 s off periods using an illumination intensity of 12 mW cm^{-2}.

precursor solutions were sonicated with a VWR Ultrasonic Bath USC300D at full power for 1 h and then degassed under 92 kPa vacuum prior to use, as void-free hydrogels are critical. Figure 3 outlines the hydrogel fabrication process. Immediately after preparation, 0.5 μL of polyacrylamide or PEG DA precursor was quickly pipetted into the microchip via the inlets. The silanized microchannels and void space in the microchip were then filled by capillary forces.

2.3.3. Illumination Procedure. The microchip was carefully aligned and brought in direct contact with a chromium photomask consisting of periodic rectangular- or square-shaped patterns (Figure 3, Figure 4 and Supporting Information, S1). An optical mask alignment system (EVG 620) or transparent tape was then used to hold the photomask and microchip together. Hydrogel precursor solution was exposed to UV light through the photomask using a mercury arc lamp with a light uniformity of 100 mm ± 2% for 365 nm wavelength and with a spectrum range of 350 to 450 nm. The UV lamp was modulated in a mask alignment system and had a software controlled mechanical shutter. The illumination intensity of the UV light source was 12 mW cm^{-2}, which was measured using a UV intensity meter. The total exposure duration was 10 min with intermittent illumination cycles (2 s on followed by 4 s off). After exposure, the non-cross-linked hydrogel precursor was removed from the main channels by vacuum suction. Images of patterned hydrogels were recorded immediately after the patterning process and processed microchips were kept in deionized water at room temperature.

3. RESULTS AND DISCUSSION

Our approach consists of polishing the upper glass layer of the microchip, injecting hydrogel precursor into the microchannels, applying optical lithography with intermittent illumination to pattern spatially defined hydrogel microstructures, and removing non-cross-linked hydrogel precursor by vacuum suction. Inside microchip, rectangular- or square-shaped glass pillars provide mechanical stabilization of microchannels and hydrogel structures, while microfluidic inlets and outlets facilitate precise control of the fluids.

3.1. Grinding and Polishing. The minimum resolution of the hydrogel structures has been shown to be directly proportional to the square root of the spacing between hydrogel precursor and photomask.[32] In our case, the spacing is determined by the upper glass layer thickness, which has to be minimized in order to improve the structure resolution. To create structures with a minimum feature size of 4 μm, it is essential to grind and polish the upper glass layer. We ground the upper glass layer to reduce its thickness from ~525 to ~100 μm, hence, the overall thickness of the microchip was reduced from 1050 to ~600 μm. It is also possible to combine a 525 μm thick upper layer with a 1000 μm thick lower layer to increase the stability of the microchip after the grinding process.

During grinding, the surface roughness increased from ~20 to 1200 nm due to the size of the silicon carbide particles. Since this roughness will cause UV light diffraction, the surface was subsequently polished to reduce the mean surface roughness to ~3 nm. Polishing improved the fidelity with which the pattern of photomask is transferred to the polymerized hydrogel. Fidelity was determined by the hydrogel structures with widths showing 90−110% similarity to the patterns on the photomask. When compared to the patterning results of a nonpolished surface, polished surface increased the fidelity ~20%. The integrity of the pattern transfer was characterized by optical microscopy and SEM Supporting Information, S1, contains examples of fabricated hydrogel structures (a) with indistinct edges when an unpolished upper layer was used, and (b) with high fidelity pattern transfer when a polished upper layer was used in the patterning process.

3.2. Surface Functionalization. In early experiments, we fabricated microarrays of polyacrylamide and PEG DA hydrogels in microchannels that had not been functionalized with an adhesion-promoting silane layer. While we could successfully pattern hydrogel microarrays using this approach, individual hydrogel structures easily detached from the glass surface when excess precursor solution was removed via vacuum suction, due to the weak surface attachment.[33] To prevent detachment, 3-trimethoxysilylpropyl methacrylate was coated on the inner walls of the microchip. The methacrylate contains unsaturated C═C functional groups which attached to the glass surface during surface functionalization.[34] When exposed to UV light, these functional groups react with radical species of the hydrogel precursor, and form covalent bonds between hydrogel and the glass surface. A detailed explanation of the silanization process and its optimization was reported by Vidič et al.[31] Surface functionalization allowed the hydrogels to attach to the glass surface during photopolymerization,[28] eliminated the detachment problems, and increased the mechanical stability of the hydrogel structures in the chip. Supporting Information, S2, shows the cross-section of a microchannel where a polyacrylamide hydrogel block was photopolymerized between two glass pillars. It can be seen that the polymerized hydrogel is in contact with both the top and bottom surfaces of the microchannel.

3.3. Optimization of Patterning Resolution. *3.3.1. Polymerization Process and the Effect of Diffusion.* Both polyacrylamide and PEG DA precursors create negative patterns upon exposure to UV light; in other words, the regions of the hydrogel precursor exposed to UV light form a cross-linked polymer network while masked regions stay non-cross-linked. In the illuminated region, photoactivation of the

DOI: 10.1021/acs.biomac.5b01104
Biomacromolecules 2015, 16, 3802−3810

photoinitiator leads to the generation of free radicals in non-cross-linked hydrogel precursor.[35] Supporting Information, S3, gives the overview of the polymerization reactions for polyacrylamide and PEG DA hydrogels. Free radicals start the cross-linking process by randomly associating with monomers and growing polymer chains, which eventually become polymerized in the illuminated region. Free radicals also diffuse from the illuminated region to the masked region due to the concentration gradient formed (Supporting Information, S4). Diffusing free radicals will lead to irregular polymerization by extending the polymerized area toward the masked region.[36] Similarly, monomers will diffuse from the masked region to the illuminated region, where they are consumed by the cross-linking reaction. Fuxman[37] and Vergote[38] showed that diffusion of monomers creates an edge overshoot at the illumination interface, by modeling hydrogel-based dosimeters with high intensity radiation doses. Since both processes are diffusion-driven, they are affected by a number of factors: (1) illumination intensity, (2) illumination wavelength, (3) the rate of production of free radicals, (4) the rate of consumption of free radicals and monomers by polymerization, (5) the diffusion rate of the free radicals toward the masked region, (6) the diffusion rate of monomers toward the illuminated region, and (7) the shape and dimensions of the photomask.[39,40] All these effects make accurate control of the structure resolution difficult.

3.3.2. Polymerization Propagation and Diffusion Rates. We optimized the polymerization rate for both polyacrylamide and PEG DA by tuning the monomer concentration, photoinitiator concentration, and diffusion rates of both monomers and cross-linkers. Two different photoinitiators with different molar absorptivities at 365 nm wavelength were also used for the two hydrogels. Polymerization and diffusion rates of polyacrylamide and PEG DA will be calculated and compared in this section.

The initiation rate for chain polymerizations, R_i, is given by[41−43]

$$R_i = \frac{2\phi\varepsilon f I C_i}{N_A h\nu} \tag{1}$$

where I is the incident light intensity (a constant 12 mW cm^{-2} is taken), C_i is the photoinitiator concentration, ε is the molar absorptivity, ϕ is the quantum yield, f is the photoinitiator efficiency, N_A is the Avagodro's number, h is the frequency of the initiating light, and ν is the speed of light. Table 1 shows the parameters used for calculations in this study.[42−46] The molar absorptivity of DMPA, the photoinitiator used for polyacrylamide, was reported as 15.000 M^{-1} m^{-1} at 365 nm wavelength under a 50 mW cm^{-2} of illumination intensity.[42] We find the initiation rate of DMPA as 0.05 mol m^{-3} s^{-1} from eq 1. For polyacrylamide, the polymerization proceeds by forming a linear network of a cross-linker and a monomer with occasional interchain cross-links (Supporting Information, S3a). The rate of chain propagation is the result of the initiation rate and the chain termination rate and in the steady state approximation is given by

$$v_p = \frac{k_p}{\sqrt{k_t}}\sqrt{\frac{R_i}{2}}[M] \tag{2}$$

where k_p is the propagation rate of the polymer, k_t its termination rate, and $[M]$ the initial monomer concentration. From eq 2, using the value for $k_p/\sqrt{k_t}$ of 3.3 (at 25 °C) reported by Curry et al.,[41] we obtain the chain propagation rate of polyacrylamide, $v_{p,PA}$ = 105 mol m^{-3} s^{-1}.

In PEG DA, every monomer is a cross-linker; however, the unsaturated C═C functional groups, which propagate the cross-linking reaction, is sterically hindered due to the neighboring methyl group (Supporting Information, S3b). Therefore, k_p of PEG DA is slightly lower than k_p of polyacrylamide. Irgacure 2959 was used as the photoinitiator of PEG DA, having a molar absorptivity of 400 M^{-1} m^{-1} at 365 nm wavelength under a 10 mW cm^{-2} of illumination intensity.[43] From eq 1 the reaction rate initiated by Irgacure 2959 was found as 0.02 mol m^{-3} s^{-1}. The chain propagation rate of PEG DA is then calculated as $v_{p,PEG\ DA}$ = 33 mol m^{-3} s^{-1} using eq 2, k_p (25 m^3 mol^{-1} s^{-1}), and k_t (2520 m^3 mol^{-1} s^{-1}) reported by Dendukiri et al.[47]

In water, the diffusion coefficients for both Irgacure 2959 and DMPA are given as 3 × 10^{-10} m^2 s^{-1} in Fang et al.,[35] while those for both acrylamide and bis are given as 4 × 10^{-10} m^2 s^{-1} in Fuxman et al.,[37] and the diffusion coefficient for PEG DA monomer is given as 1.5 × 10^{-11} m^2 s^{-1} in Harada et al.[48] When monomers and free radicals are consumed by the polymerization reaction in the illuminated region, a concentration gradient is formed. Fick's second law gives the resulting concentration changes:

$$\frac{dC}{dt} = D\frac{d^2C}{dx^2} \tag{3}$$

where D is the diffusion coefficient, C is the concentration of monomers, t is the time scale, and x is the direction normal to the illuminated region. From eq 3, we calculate the concentration difference over a distance of 10 μm (that is the distance between the midpoint of the illuminated region and the border of the masked region), when $dC/dt = 0$ (i.e., when diffusional monomer supply to the illuminated region is in balance with the monomer consumption in this region). We find the generated concentration difference is 26 mol m^{-3} and 33 mol m^{-3} for polyacrylamide and PEG DA, respectively. Both values are comparable to the initial monomer concentrations, which are 400 mol m^{-3} and 100 mol m^{-3} for polyacrylamide and PEG DA, respectively. For both polymers, a continuous 12 mW cm^{-2} illumination intensity is therefore too high as it depletes monomers and will cause diffusion of free radicals to the masked region.

3.3.3. Illumination Recipe. Intermittent illumination technique was previously used to fabricate single hydrogel membranes using solid state and pulsed UV laser setups.[49,50] In our case, the intermittent illumination strategy was chosen due to the limitations of our equipment that does not allow for using a neutral density filter or changing the light intensity. The

Table 1. Parameters Used in This Study[a]

parameter	value for DMPA	value for Irgacure 2959	units	source
ε	15000	400	M^{-1} m^{-1}	42, 43
ϕ	1	0.3		44, 45
f	0.6	0.5		46
I	120	120	W cm^{-2}	this work
C_i	400	100	mol m^{-3}	this work

[a]These values were used to calculate R_i and propagation rates. The different sources in the literature used to collect the values are indicated in the rightmost column.

DOI: 10.1021/acs.biomac.5b01104
Biomacromolecules 2015, 16, 3802−3810

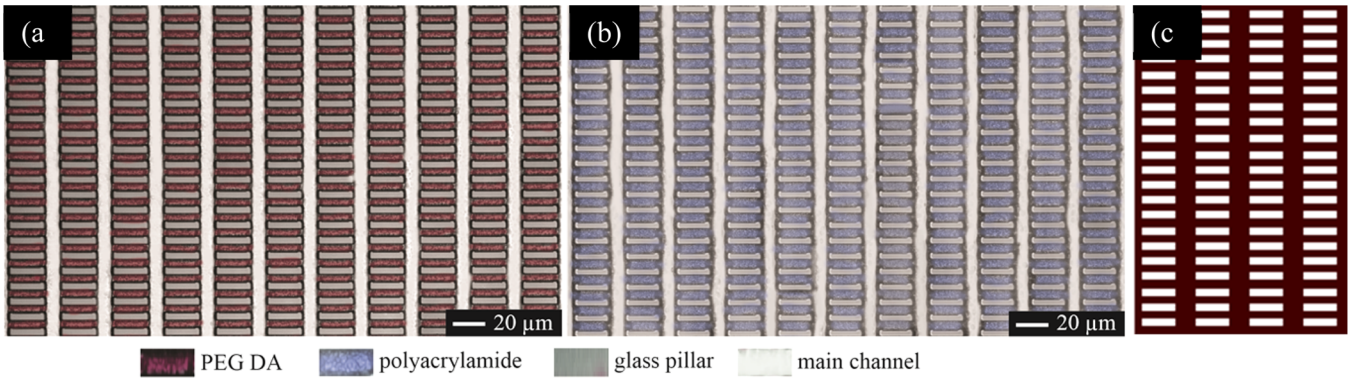

Figure 5. Phase contrast microscopy images of photopolymerized (a) PEG DA and (b) polyacrylamide hydrogels. The images are artificially colored on the basis of gray scale differences. (c) The photomask used in photopolymerization.

Table 2. Comparison of Hydrogel Polymerization Times between 1 mL Tubes and Microchips[a]

(a) Polyacrylamide			
		UV exposure[b]	
monomer concentration (%T)	DMPA (%)	polymerization in tube (V = 1 mL)	polymerization in microchip (V = 0.5 μL)
2	2	NP	NP
2.5	2	1.5 ± 0.5 min	NP
4	2	20 ± 10.4 s	10 ± 1.1 min
6	2	15 ± 5.6 s	8.5 ± 1.4 min
8	2	10 ± 4.3 s	8 ± 1.0 min
(b) PEG DA			
		UV exposure[b]	
monomer concentration (%)	Irgacure (%)	polymerization in tube (V = 1 mL)	polymerization in microchip (V = 0.5 μL)
5	10	NP	NP
10	10	6 ± 1.4 min	NP
15	10	3 ± 0.5 min	10 ± 0.8 min
20	10	1 ± 0.2 min	8 ± 0.8 min

[a]The results present the mean and standard error deviations, $n \geq 3$. NP: no polymerization or partial polymerization longer than an overnight. [b]UV exposure was applied at 365 nm, with 12 mW cm^{-2} intensity, and using intermittent illumination cycles (2 s on followed by 4 s off).

dark period of 4 s was chosen to maintain the diffusional relaxation time over 10 μm distance for PEG DA monomers, which is 3.3 s. The dark period was then combined with an illumination period of 2 s since high resolution patterning results were obtained for both hydrogels in this illumination scheme. In contrast to intermittent illumination, continuous illumination (see section 3.3.6) was found to lead polymerization in the entire chip.

We also investigated possible temperature changes during polymerization. Supporting Information, S5, demonstrates the temperature change of the microchip during the intermittent illumination and flood illumination. The results show that the temperature rise due to UV absorption was 0.5 °C after 10 min of intermittent illumination (2 s on followed by 4 s off), while it was ∼3 °C after 10 min of continuous illumination. Since the illumination intensity was as low as 12 mW cm^{-2} in our study, only small temperature gradients were apparently formed in the microchip, leading to trivial changes (∼5%) in the diffusion fluxes.

Using the intermittent illumination approach, hydrogel patches were successfully patterned between glass pillars and remained separated from each other in both horizontal and vertical directions. Figure 4 illustrates the difference between hydrogel patterns fabricated using intermittent illumination cycles and continuous exposure. Longer UV illumination periods were found to increase the width of the hydrogel features and reduced the patterning resolution. Figure 5 shows arrays of polyacrylamide and PEG DA structures fabricated using intermittent illumination.

3.3.4. Photoinitiator and Monomer Concentrations. In addition to polishing the upper glass layer and applying an intermittent illumination recipe, we studied the influence of the initial photoinitiator and monomer concentrations on the patterning success. We used DMPA and Irgacure 2959 photoinitiators to cross-link polyacrylamide and PEG DA hydrogels, respectively. We observed that varying the photoinitiator concentration did not affect the patterning resolution (Supporting Information, S6). Liu et al.[29] reported a similar result, suggesting that the resolution of hydrogel structures is independent of the initial photoinitiator concentration. We also observed that polyacrylamide and PEG DA precursor solutions did not cross-link at concentrations lower than 2% (v/v) of DMPA and 10% (v/v) of Irgacure 2959, respectively.

In contrast, photopolymerization time, which is needed to cross-link all the precursor in the illuminated region, and structure resolution were found to be dependent on initial monomer concentration. Under intermittent illumination, we observed that the polymerization time decreases with increasing monomer concentration, resulting in well-defined but highly dense hydrogel structures. Reducing the monomer concen-

DOI: 10.1021/acs.biomac.5b01104
Biomacromolecules 2015, 16, 3802−3810

tration led to structures with indistinct edges and a softer texture probably due to the formation of the hydrogel with a larger pore size. Table 2 summarizes the relation between monomer concentration and polymerization time for both hydrogel types in Eppendorf tubes and microchips. It is thereby important to note that polymerization was observed to take longer time in the microchip (with a volume of 0.5 μL) compared to polymerization in the large volume Eppendorf tube (with a volume of 1 mL). Polyacrylamide has been observed to fail cross-linking below 2.5%T (%T refers to the total mass of monomer) in both Eppendorf tubes and microchips,[35] while PEG DA fails cross-linking at 5% concentration and below.

3.3.5. Patterning Success Evaluation. The patterning success was evaluated based on the similarity between the hydrogel patterns in the microchannels and structures on the photomask. Similarity was defined as actual hydrogel size relative to the structures on the photomask expressed as percentage. Three representative images were collected from two opposite corners and a middle section of the arrays, each containing 250 hydrogel subunits.

Hydrogel structures with 90−110% similarity were considered successful, while structures with less similarity or indistinct edges were considered failures. Hydrogel patterns larger than 110% and smaller than 90% of the photomask structures were not observed when intermittent illumination recipe was applied. Patterning success and resolution were found to improve for small feature sizes with a thinner glass cover thickness for both polyacrylamide and PEG DA hydrogels, as shown in Table 3.

Table 3. Patterning Success vs Upper Glass Layer Thickness[a]

	polyacrylamide		PEG DA	
upper layer thickness (μm)	patterning success (%)	std deviation (%)	patterning success (%)	std deviation (%)
100	98.5	0.8	98.7	1.0
115	94.9	4.5	95.5	4.7
250	37.7	10.6	20.0	10.3
400	0	0	0	0
525	0	0	0	0

[a]The results present the mean and standard error deviations, n = 2. Approximate values are given for the upper layer thicknesses.

Upper glass layer thicknesses larger than 115 μm were not suitable for patterning feature sizes of 4 μm, hydrogel structures could not be obtained with thicknesses of 250, 400, and 525 μm, regardless of the UV exposure time.

We also investigated the possibility that the size of the features after photopolymerization could be impacted by swelling or shrinking of the hydrogels after evacuating the microchip, or after changing aqueous media conditions. To achieve this, we compared the volume changes of hydrogels just after the fabrication (when the surrounding environment was dry) and after 24 h in aqueous media. Swelling ratios were found as 1−2% for polyacrylamide and 5−6% for PEG DA. Since both of the hydrogels are of zero net charge, the swelling or shrinking behavior was not substantial.

With these fabrication and processing techniques, we successfully patterned 0.4 × 10^6 per cm^2 hydrogel structures, each with ∼1.25 pL volume, with a ∼98.5% patterning success using both polyacrylamide and PEG DA hydrogels.

3.3.6. Other Illumination Strategies. The hydrogel precursor was exposed to continuous illumination for 1, 3, 5, 7, and 10 min. While partial polymerization (∼15% of the precursor volume) was observed after 1 min, a faithful reproduction was obtained by 3 min of exposure. The energy of 3 min exposure is equal to approximately 10 min intermittent illumination (2 s on followed by 4 s off cycles). In continuous illumination cases, except for 1 min, photomask patterns could not be transferred to the microchip. Figure 4a demonstrates the polymerization after 10 min of continuous illumination. In Figure 4b, hydrogel arrays contain defect-free subunits with no hydrogel precursor residue remaining in the main channels. The same image shows the polymerization result for intermittent illumination for 10 min, before which hydrogel patterns were not fully polymerized.

A couple of more strategies could further reduce the feature size; that is, increasing the distance between the hydrogel structures, using a thinner upper layer, reducing the illumination intensity, and shortening the exposure times. However, the spatial resolution of the microstructures will be limited by UV light diffraction, diffusion of hydrogel components, and wavelength of the UV light.

4. CONCLUSIONS

In this work, we demonstrated a simple and reproducible photopatterning process for micron-sized hydrogel arrays inside a closed microchip. Fabricating periodic hydrogel microarrays in polished microchips by optical lithography is preferable to the vast majority of previously demonstrated patterning methods because of the sub-10 μm sized features, improved resolution, and high reproducibility. However, while capillary pinning method provides the patterning of both photopolymerizing and thermogelling hydrogels, only photopolymerizing ones can be patterned using the present technique.

This technique is based on mechanically polishing the top glass layer to reduce the spacing between the photomask and hydrogel precursor, and applying intermittent illumination for enhancing the definition of hydrogel boundaries. Microfluidic networks consisting of 0.4 × 10^6 periodic picoliter-volume hydrogel patterns can easily be patterned over 1 cm^2 areas with ∼1.5% failures. We experimentally showed that upper glass layer thickness, monomer concentration, and different optical lithography recipes have a significant effect on structure resolution. By tuning these parameters, a minimum feature size of 4 μm was patterned using both polyacrylamide and PEG DA 3400 hydrogels. Using this method, various shapes and thicknesses of periodic hydrogel structures can be patterned by adjusting the pillar size, pillar shape, and channel depth. This simple and effective fabrication strategy allows for direct integration of hydrogel microarrays into microfluidic systems. It further holds great potential in the fabrication of 3-D hydrogel matrices for elucidation of fundamental structure−function relationships,[48] biomolecule separation,[49] biosensing,[50] tissue engineering,[51] immobilized protein microarrays,[52] subdivided-hydrogel microarrays for bacteria cultures,[53] and 3D cell cultures.[15]

■ ASSOCIATED CONTENT

Supporting Information

The Supporting Information is available free of charge on the ACS Publications website at DOI: 10.1021/acs.biomac.5b01104.

DOI: 10.1021/acs.biomac.5b01104
Biomacromolecules 2015, 16, 3802−3810

Phase contrast microscopy images of photopolymerized polyacrylamide hydrogel, photomask patterns used in photopolymerization, scanning electron micrograph of a polyacrylamide hydrogel block that is polymerized between two glass pillars, polymerization reactions of polyacrylamide and PEG DA, a schematic diagram of the cross-linking reaction in the hydrogel under high and low intensity UV illumination, and temperature profile of the microchip when intermittent illumination and continuous illumination were applied (PDF).

AUTHOR INFORMATION

Corresponding Authors

*E-mail: b.gumuscu@utwente.nl. Phone: +31 053489 4580.
*E-mail: j.c.t.eijkel@utwente.nl. Phone: +31 053489 2839.

Notes

The authors declare no competing financial interest.

ACKNOWLEDGMENTS

This work was funded by the Dutch network for Nanotechnology NanoNext NL, in the subprogram "Nanofluidics for Lab-on-a-Chip". Authors thank Roy Kooijman for helping in microchip fabrication, and Allison C. E. Bidulock and Mark A. Hempenius for thorough discussions. Authors also thank the anonymous referees and Molly Shoichet for their valuable comments that helped us to improve the quality of this work.

REFERENCES

(1) Peppas, N. A.; Hilt, J. Z.; Khademhosseini, A.; Langer, R. Hydrogels in Biology and Medicine: From Molecular Principles to Bionanotechnology. *Adv. Mater.* **2006**, *18* (11), 1345−1360.

(2) Park, T. G. Temperature Modulated Protein Release from Ph/Temperature-Sensitive Hydrogels. *Biomaterials* **1999**, *20* (6), 517−521.

(3) Grassi, G.; Farra, R.; Caliceti, P.; Guarnieri, G.; Salmaso, S.; Carenza, M.; Grassi, M. Temperature-Sensitive Hydrogels. *Am. J. Drug Delivery* **2005**, *3* (4), 239−251.

(4) Tanaka, T. Collapse of Gels and the Critical Endpoint. *Phys. Rev. Lett.* **1978**, *40* (12), 820.

(5) Li, H.; Yuan, Z.; Lam, K. Y.; Lee, H. P.; Chen, J.; Hanes, J.; Fu, J. Model Development and Numerical Simulation of Electric-Stimulus-Responsive Hydrogels Subject to an Externally Applied Electric Field. *Biosens. Bioelectron.* **2004**, *19* (9), 1097−1107.

(6) Charati, M. B.; Lee, I.; Hribar, K. C.; Burdick, J. A. Light-Sensitive Polypeptide Hydrogel and Nanorod Composites. *Small* **2010**, *6* (15), 1608−1611.

(7) Tanaka, T.; Nishio, I.; Sun, S. T.; Ueno-Nishio, S. Collapse of Gels in an Electric Field. *Science* **1982**, *218* (4571), 467−469.

(8) Guan, T.; Godts, F.; Ceyssens, F.; Vanderleyden, E.; Adesanya, K.; Dubruel, P.; Neves, H. P.; Puers, R. Development and Fabrication of a Novel Photopatternable Electric Responsive Pluronic Hydrogel for MEMS Applications. *Sens. Actuators, A* **2012**, *186*, 184−190.

(9) Reddy, S. M.; Phan, Q. T.; El-Sharif, H.; Govada, L.; Stevenson, D.; Chayen, N. E. Protein Crystallization and Biosensor Applications of Hydrogel-Based Molecularly Imprinted Polymers. *Biomacromolecules* **2012**, *13* (12), 3959−3965.

(10) Paustian, J. S.; Azevedo, R. N.; Lundin, S. T. B.; Gilkey, M. J.; Squires, T. M. Microfluidic Microdialysis: Spatiotemporal Control over Solution Microenvironments using Integrated Hydrogel Membrane. Microwindows. *Phys. Rev. X* **2013**, *3* (4), 041010.

(11) Koh, W. G.; Pishko, M. V. Fabrication of Cell-Containing Hydrogel Microstructures Inside Microfluidic Devices That Can Be Used As Cell-Based Biosensors. *Anal. Bioanal. Chem.* **2006**, *385* (8), 1389−1397.

(12) Ashley, G. W.; Henise, J.; Reid, R.; Santi, D. V. Hydrogel Drug Delivery System with Predictable and Tunable Drug Release and Degradation Rates. *Proc. Natl. Acad. Sci. U. S. A.* **2013**, *110* (6), 2318−2323.

(13) Byun, J. Y.; Lee, K. H.; Lee, K. Y.; Kim, M. G.; Kim, D. M. In-Gel Expression and in situ Immobilization of Proteins for Generation of Three Dimensional Protein Arrays in a Hydrogel Matrix. *Lab Chip* **2013**, *13* (5), 886−891.

(14) Suzuki, A.; Tanaka, T. Phase Transition in Polymer Gels Induced by Visible Light. *Nature* **1990**, *346* (6282), 345−347.

(15) Rubina, A. Y.; Kolchinsky, A.; Makarov, A. A.; Zasedatelev, A. S. Why 3-D? Gel-Based Microarrays in Proteomics. *Proteomics* **2008**, *8* (4), 817−831.

(16) Fernandes, T. G.; Diogo, M. M.; Clark, D. S.; Dordick, J. S.; Cabral, J. M. High-Throughput Cellular Microarray Platforms: Applications in Drug Discovery, Toxicology and Stem Cell Research. *Trends Biotechnol.* **2009**, *27* (6), 342−349.

(17) Lee, J. Y.; Shah, S. S.; Yan, J.; Howland, M. C.; Parikh, A. N.; Pan, T.; Revzin, A. Integrating Sensing Hydrogel Microstructures into Micropatterned Hepatocellular Cocultures. *Langmuir* **2009**, *25* (6), 3880−3886.

(18) Hahn, M. S.; Miller, J. S.; West, J. L. Three-Dimensional Biochemical and Biomechanical Patterning of Hydrogels for Guiding Cell Behavior. *Adv. Mater.* **2006**, *18* (20), 2679−2684.

(19) Di Benedetto, F.; Biasco, A.; Pisignano, D.; Cingolani, R. Patterning Polyacrylamide Hydrogels by Soft Lithography. *Nanotechnology* **2005**, *16* (5), S165.

(20) Kaehr, B.; Shear, J. B. Multiphoton Fabrication of Chemically Responsive Protein Hydrogels for Microactuation. *Proc. Natl. Acad. Sci. U. S. A.* **2008**, *105* (26), 8850−8854.

(21) Suh, K. Y.; Seong, J.; Khademhosseini, A.; Laibinis, P. E.; Langer, R. A Simple Soft Lithographic Route to Fabrication of Poly (Ethylene Glycol) Microstructures for Protein and Cell Patterning. *Biomaterials* **2004**, *25* (3), 557−563.

(22) Zhao, L.; Lee, V. K.; Yoo, S. S.; Dai, G.; Intes, X. The Integration Of 3-D Cell Printing and Mesoscopic Fluorescence Molecular Tomography of Vascular Constructs within Thick Hydrogel Scaffolds. *Biomaterials* **2012**, *33* (21), 5325−5332.

(23) Peng, J.; Zhao, D.; Tang, X.; Tong, F.; Guan, L.; Wang, Y.; Zhang, M.; Cao, T. Cool Microcontact Printing to Fabricate Thermosensitive Microgel Patterns. *Langmuir* **2013**, *29* (38), 11809−11814.

(24) Eng, G.; Lee, B. W.; Parsa, H.; Chin, C. D.; Schneider, J.; Linkov, G.; Sia, S. K.; Vunjak-Novakovic, G. Assembly of Complex Cell Microenvironments Using Geometrically Docked Hydrogel Shapes. *Proc. Natl. Acad. Sci. U. S. A.* **2013**, *110* (12), 4551−4556.

(25) Jiang, X.; Ng, J. M.; Stroock, A. D.; Dertinger, S. K.; Whitesides, G. M. A Miniaturized, Parallel, Serially Diluted Immunoassay for Analyzing Multiple Antigens. *J. Am. Chem. Soc.* **2003**, *125* (18), 5294−5295.

(26) Helgeson, M. E.; Chapin, S. C.; Doyle, P. S. Hydrogel Microparticles from Lithographic Processes: Novel Materials for Fundamental and Applied Colloid Science. *Curr. Opin. Colloid Interface Sci.* **2011**, *16* (2), 106−117.

(27) Guan, T.; Ceyssens, F.; Puers, R. Fabrication and Testing of a Mems Platform for Characterization of Stimuli-Sensitive Hydrogels. *J. Micromech. Microeng.* **2012**, *22* (8), 087001.

(28) Hahn, M. S.; Taite, L. J.; Moon, J. J.; Rowland, M. C.; Ruffino, K. A.; West, J. L. Photolithographic Patterning of Polyethylene Glycol Hydrogels. *Biomaterials* **2006**, *27* (12), 2519−2524.

(29) Liu, H.; Zhao, W.; Hao, X.; Redshaw, C.; Huang, W.; Sun, W. H. 2, 6-Dibenzhydryl-N-(2-Phenyliminoacenaphthylenylidene)-4-methylbenzenamine Nickel Dibromides: Synthesis, Characterization, and Ethylene Polymerization. *Organometallics* **2011**, *30* (8), 2418−2424.

(30) Gumuscu, B.; Bomer, J. G.; van den Berg, A.; Eijkel, J. C. T. Large Scale Patterning of Hydrogel Microarrays Using Capillary Pinning. *Lab Chip* **2015**, *15* (3), 664−667.

DOI: 10.1021/acs.biomac.5b01104
Biomacromolecules 2015, 16, 3802−3810

(31) Vidič, J.; Podgornik, A.; Štrancar, A. Effect of the Glass Surface Modification on the Strength of Methacrylate Monolith Attachment. *J. Chrom. A* **2005**, *1065* (1), 51−58.
(32) Gandhi, S. K. *VLSI Fabrication Principles: Silicon and Gallium Arsenide*; John Wiley: New York, 1994; Vol. *117*.
(33) Revzin, A.; Russell, R. J.; Yadavalli, V. K.; Koh, W. G.; Deister, C.; Hile, D. D.; Mellott, M. B.; Pishko, M. V. Fabrication of Poly (Ethylene Glycol) Hydrogel Microstructures Using Photolithography. *Langmuir* **2001**, *17* (18), 5440−5447.
(34) Seong, G. H.; Zhan, W.; Crooks, R. M. Fabrication of Microchambers Defined by Photopolymerized Hydrogels and Weirs Within Microfluidic Systems: Application to DNA Hybridization. *Anal. Chem.* **2002**, *74* (14), 3372−3377.
(35) Scott, T. F.; Kowalski, B. A.; Sullivan, A. C.; Bowman, C. N.; McLeod, R. R. Two-Color Single-Photon Photoinitiation and Photoinhibition for Subdiffraction Photolithography. *Science* **2009**, *324* (5929), 913−917.
(36) Hou, C.; Herr, A. E. Ultrashort Separation Length Homogeneous Electrophoretic Immunoassays Using On-Chip Discontinuous Polyacrylamide Gels. *Anal. Chem.* **2010**, *82* (8), 3343−3351.
(37) Fuxman, A. M.; McAuley, K. B.; Schreiner, L. J. Modelling of Polyacrylamide Gel Dosimeters with Spatially Non-Uniform Radiation Dose Distributions. *Chem. Eng. Sci.* **2005**, *60* (5), 1277−1293.
(38) Vergote, K.; De Deene, Y.; Bussche, E. V.; De Wagter, C. On the Relation Between the Spatial Dose Integrity and the Temporal Instability of Polymer Gel Dosimeters. *Phys. Med. Biol.* **2004**, *49* (19), 4507.
(39) Pollak, A.; Blumenfeld, H.; Wax, M.; Baughn, R. L.; Whitesides, G. M. Enzyme Immobilization by Condensation Copolymerization into Crosslinked Polyacrylamide Gels. *J. Am. Chem. Soc.* **1980**, *102* (20), 6324−6336.
(40) Fang, N.; Sun, C.; Zhang, X. Diffusion-Limited Photopolymerization in Scanning Micro-Stereolithography. *Appl. Phys. A: Mater. Sci. Process.* **2004**, *79* (8), 1839−1842.
(41) Currie, D. J.; Dainton, F. S.; Watt, W. S. The Effect of pH on the Polymerization Rate of Acrylamide in Water. *Polymer* **1965**, *6* (9), 451−453.
(42) Berchtold, K. A.; Lovell, L. G.; Nie, J.; Hacioğlu, B.; Bowman, C. N. The Significance of Chain Length Dependent Termination in Cross-linking Polymerizations. *Polymer* **2001**, *42* (11), 4925−4929.
(43) Fairbanks, B. D.; Schwartz, M. P.; Bowman, C. N.; Anseth, K. S. Photoinitiated Polymerization of PEG-diacrylate with Lithium Phenyl-2, 4, 6-trimethylbenzoylphosphinate: Polymerization Rate and Cytocompatibility. *Biomaterials* **2009**, *30* (35), 6702−6707.
(44) Bitsch, B.; Barner-Kowollik, C.; Zhu, S. Modeling the Effects of Reactor Backmixing on RAFT Polymerization. *Macromol. React. Eng.* **2011**, *5* (1), 55−68.
(45) Liu, M.; Li, M. D.; Xue, J.; Phillips, D. L. Time-Resolved Spectroscopic and Density Functional Theory Study of the Photochemistry of Irgacure-2959 in an Aqueous Solution. *J. Phys. Chem. A* **2014**, *118* (38), 8701−8707.
(46) Lalevee, J.; El-Roz, M.; Allonas, X.; Fouassier, J. P. Controlled Photopolymerization Reactions: The Reactivity of New Photoiniferters. *J. Polym. Sci., Part A: Polym. Chem.* **2007**, *45* (12), 2436−2442.
(47) Dendukuri, D.; Panda, P.; Haghgooie, R.; Kim, J. M.; Hatton, T. A.; Doyle, P. S. Modeling of Oxygen-Inhibited Free Radical Photopolymerization in a PDMS Microfluidic Device. *Macromolecules* **2008**, *41* (22), 8547−8556.
(48) Harada, A.; Kataoka, K. Formation of Polyion Complex Micelles in an Aqueous Milieu from a Pair of Oppositely-Charged Block Copolymers with Poly (ethylene glycol) Segments. *Macromolecules* **1995**, *28* (15), 5294−5299.
(49) Song, S.; Singh, A. K.; Shepodd, T. J.; Kirby, B. J. Microchip Dialysis of Proteins using in situ Photopatterned Nanoporous Polymer Membranes. *Anal. Chem.* **2004**, *76* (8), 2367−2373.
(50) Liu, P.; Meagher, R. J.; Light, Y. K.; Yilmaz, S.; Chakraborty, R.; Arkin, A. P.; Hazen, T. C.; Singh, A. K. Microfluidic Fluorescence in situ Hybridization and Flow Cytometry (μFlowFISH). *Lab Chip* **2011**, *11* (16), 2673−2679.
(51) Mauck, R. L.; Seyhan, S. L.; Ateshian, G. A.; Hung, C. T. Influence of Seeding Density and Dynamic Deformational Loading on the Developing Structure/Function Relationships of Chondrocyte-Seeded Agarose Hydrogels. *Ann. Biomed. Eng.* **2002**, *30* (8), 1046−1056.
(52) Tokarev, I.; Minko, S. Stimuli-Responsive Porous Hydrogels at Interfaces for Molecular Filtration, Separation, Controlled Release, and Gating in Capsules and Membranes. *Adv. Mater.* **2010**, *22* (31), 3446−3462.
(53) Russell, R. J.; Pishko, M. V.; Gefrides, C. C.; McShane, M. J.; Cote, G. L. A Fluorescence-Based Glucose Biosensor Using Concanavalin A and Dextran Encapsulated in a Poly (Ethylene Glycol) Hydrogel. *Anal. Chem.* **1999**, *71* (15), 3126−3132.

DOI: 10.1021/acs.biomac.5b01104
Biomacromolecules 2015, 16, 3802−3810